This special edition of GEOPHYSICS Bright Spots summarizes selected articles from the July-August "Seismic Interferometry" supplement and a single article from a previous issue. Because of the singular focus of the supplement and because this is perhaps a new topic for you, this column is more tutorial than customary.

Virtual source. The creation of a virtual source is a key result of seismic interferometry. If we record traces at two locations from a wide selection of source locations, we can create from the recorded seismic data alone a trace at either of those receiver locations that appears as if the source were at the other location. It is as if we moved a source to one of the receiver locations and thus created a new virtual-source location.

We can do this without knowing the velocity structure of the medium or the locations of the true sources. (Notice that this claim is not the same as the reciprocity theorem, which observes that we can interchange the source and receiver positions and record the same total wavefield as long as there is no directionality at the source or receiver.)

The GEOPHYSICS articles in the supplement on seismic interferometry answer the questions of whether virtual sources work, how to create the virtual-sourced traces, and how to use this method. They also expand on the surprising new field of virtual sources.

In addition to this column, this issue of *TLE* contains a review article, "Seismic interferometry—turning noise into signal," and an article about its application to seismic waves traveling through a building, "Seismic anisotropy of a building."

Motivation first. Starting with the simplest question, "How can virtual sources be used?", consider the determination of the Rayleigh-wave velocity in the near surface of California. In the GEOPHYSICS supplement, Larose et al. use measured wavefields from a grid of California earthquake-monitoring stations (Figure 1) to create new measured wavefields at each receiver location as if each other receiver location were an impulsive source location. With this, Figure 1 becomes a map of receiver locations and virtual-source locations in all possible combinations between sources and receivers.

Figure 2 shows the result of the tomographic Rayleigh-wave velocity inversion, obtained from the synthesized virtual-source observations. These estimated Rayleigh-wave velocities correspond to known significant geologic features. Impressively, with the random noise of the ocean as the energy source, the method produced believable (and not random) results.

The key to creating Figure 2 was the creation of new time series at one receiver location as if a second receiver location were the location of an impulsive source, a virtual source. The authors create the desired time series by cross-correlating the recorded time series for locations A and B, creating a new virtual-source time series as if the source were at A and the receiver at B and, through reciprocity, vice versa.

Seismic interferometry. The creation of virtual sources through crosscorrelation falls within the definition of seismic interferometry. To quote Wapenaar's paper, "Following Schuster (2001), we use the term *seismic interferometry* for the process of generating new seismic responses by crosscorrelating seismic observations at different receiver locations." Now we find out how it works for the creation of virtual sources.

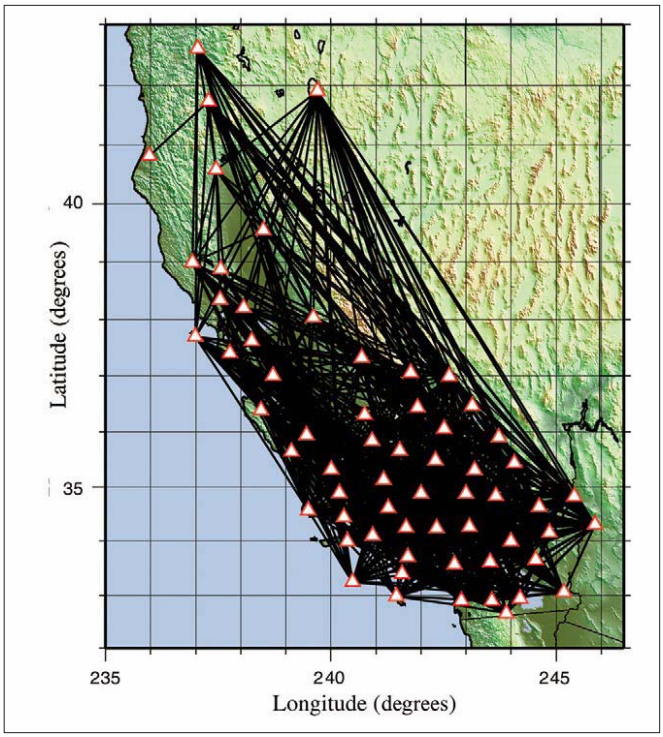

Figure 1. *Black lines show possible connecting paths for a California grid of earthquake monitoring stations. (Figure 6, Larose et al., "Correlation of random wavefields: An interdisciplinary review.")*

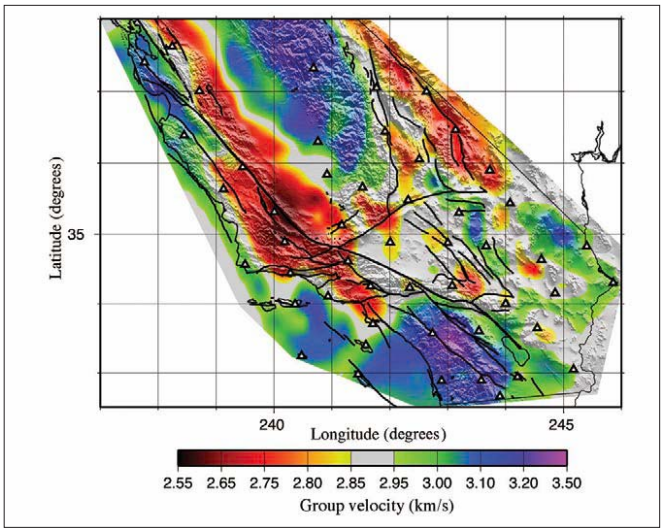

Figure 2. *Rayleigh-wave group velocity obtained from tomographic inversion. (Figure 7, Larose et al., "Correlation of random wavefields: An interdisciplinary review.")*

Huygens' principle. Using the geometry shown in the upper part of Figure 3, van Wijk simultaneously measured wavefields at two locations (x and x') on a granite slab in the laboratory. The solid raypaths contribute to the observations at both x and x'. The dotted raypath represents paths that contribute only to the observations at x. Using Huygens' principle, each location acts like a new source. Thus, we may

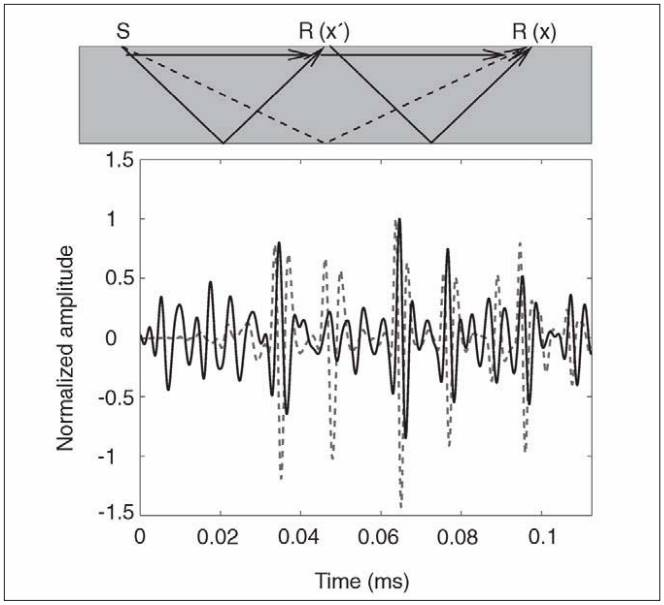

Figure 3. *Laboratory configuration (top) and comparison of recorded wave with source at x′, receiver at x (dotted line), and crosscorrelation of recorded waves with source to left of receivers at x′ and x. (Figure 3, van Wijk, "On estimating the impulse response between receivers in a controlled ultrasonic experiment.")*

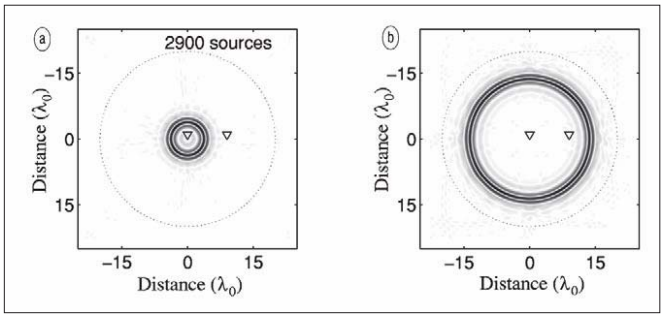

Figure 4. *Wavefield synthesized through crosscorrelation technique. The outer ring of light dots represents the lateral locations of the ring of sources. (Figure 1, Larose et al., "Correlation of random wavefields: An interdisciplinary review.")*

view the measured wavefield at x' as the source for the solid raypaths recorded at location x.

Similar to a vibroseis correlation, van Wijk correlates the seismic data recorded at x' with that recorded at x to remove the Huygens' wavelet source signature at x'. He shows the result of crosscorrelation as the solid curve in Figure 3. That crosscorrelation is the virtual-source trace.

For comparison, the dotted curve is the trace obtained from a laboratory measurement with a source at x' and the receiver at x. We will call that curve the $S(x')$ trace. The curves are not identical (normalized crosscorrelation coefficient equals 0.65) because there are rays from S to $R(x)$ that were not recorded by $R(x')$. The author expands the experiment by placing an additional 39 sources in a line, all to the left of the two receiver locations.

The author then sums (stacks) the individual crosscorrelations between $R(x)$ and $R(x')$ obtained from the 40 virtual-source traces, obtaining an improved virtual-source trace. This summation emphasizes the contributions of the raypaths seen by both $R(x')$ and $R(x)$, increasing the normalized crosscorrelation between the improved virtual-source trace and the $S(x')$ trace to 0.87. Thus, the summation of the crosscorrelations of the traces obtained at $R(x')$ and $R(x)$ is almost identical (crosscorrelation coefficient equals

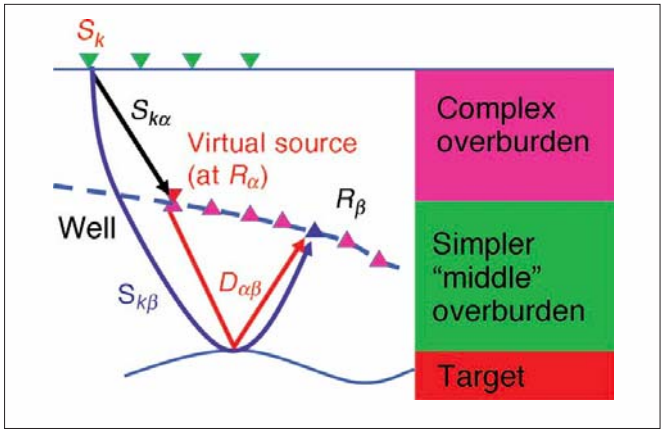

Figure 5. *Near-horizontal VSP above target reservoir. (Figure 2, Bakulin and Calvert, "The virtual source method: Theory and case study.")*

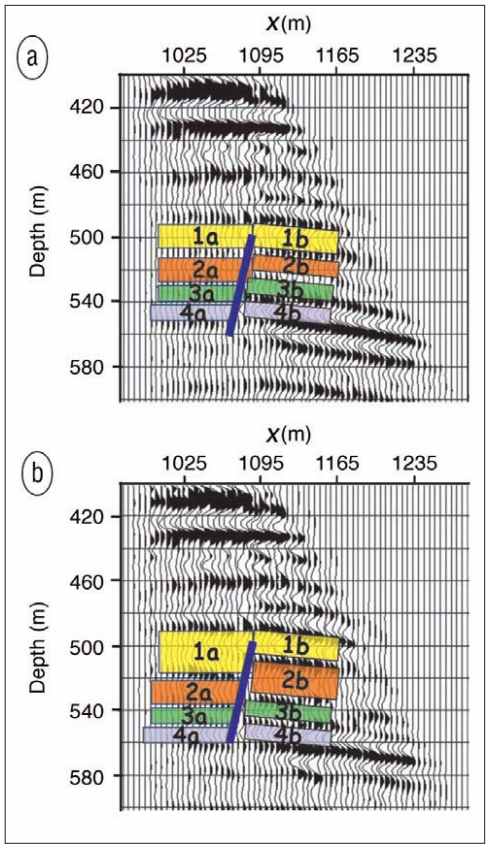

Figure 6. *Time-lapse comparison of reservoir images obtained by migrating virtual-source VSP data. Baseline survey (top) and monitor survey (bottom). (Figure 19, Bakulin and Calvert, "The virtual source method: Theory and case study.")*

0.87) to the trace with a source at x' measured by $R(x)$. The crosscorrelation technique creates a virtual source at x', assuming that the wavefield recorded at x', through Huygens' principle, provides the source signature at x'.

Notice that in apparently moving the source from its true location to create a virtual source at location x', van Wijk did not have to know the velocity of the medium. The required velocity information is encoded in the two recorded traces, at locations $R(x)$ and $R(x')$. For the same reason, the author did not have to know the locations of the true sources.

Although this example contained only two isolated reflectors (top and base of granite slab), the method requires no information about reflector locations or characteristics.

Virtual-source test. To test the ability to create virtual-source traces, Larose et al. first create a 2D wave-equation model.

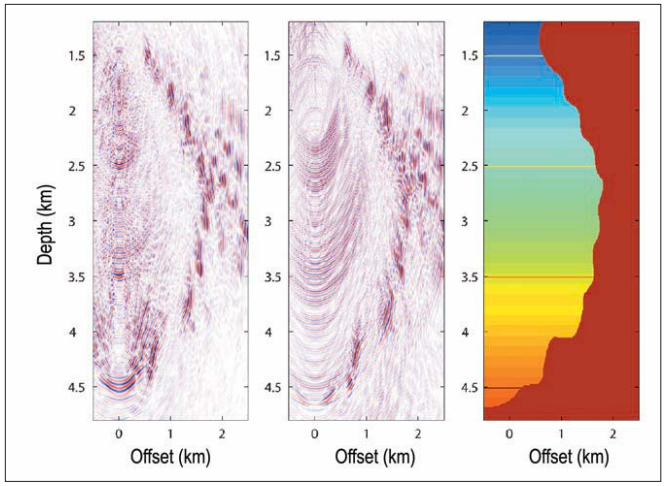

Figure 7. *Salt-face images produced from model downhole data: left, from downhole source and receiver model data; center, from surface-source, downhole receiver model data converted to virtual-source data; right, velocity model of salt wall. (Figure 4, Willis et al., "A novel application of time-reversed acoustics: Salt-dome flank imaging using walkaway VSP surveys.")*

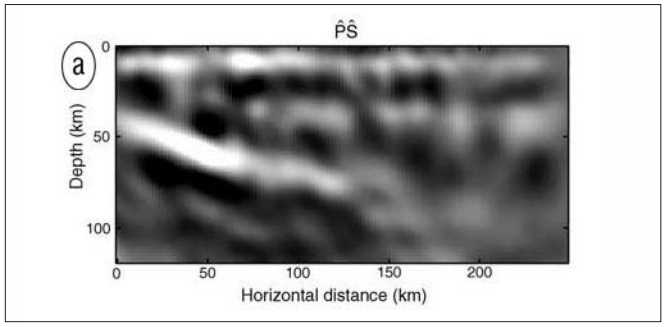

Figure 8. *P-S image of plate subducting beneath Oregon. (Figure 8a, Shragge et al., "Teleseismic shot-profile migration.")*

A ring of sources surrounds a central receiver line. For each independent source location, the authors measure the wavefield at numerous locations within the ring of possible source locations. To create wavefield measurements for a single virtual source at the model's center, the authors summed the crosscorrelations of each trace and the trace recorded at that central location. For this central source, the *x-y-t* volume of the crosscorrelations should reveal a cone-shaped event.

In Figure 4, we see this cone in two time slices, demonstrating that the volume of crosscorrelations properly recreates a central source, using only data obtained from a cylinder of source locations. Larose et al. go beyond verification of the virtual-source method by investigating its robustness for data obtained from a partial ring of sources. If the medium contains a uniformly random distribution of scatters, the scatterers act as new sources, providing a full-angle illumination allowing for an accurate reconstruction of data for a central virtual source. Minus the scatterers, the authors obtain only a partial reconstruction.

Improved reservoir monitoring. This example and others to follow further demonstrate that sources need not surround receivers to provide adequate virtual-source data. Bakulin and Calvert use the VSP geometry shown in Figure 5. Through the virtual-source method, they obtain a clearer image of the differential compaction of the reservoir across a fault (Figure 6) with a virtual source at the well location, avoiding the complex raypaths from the surface to that well. Unlike moving the source from the surface to the wellbore

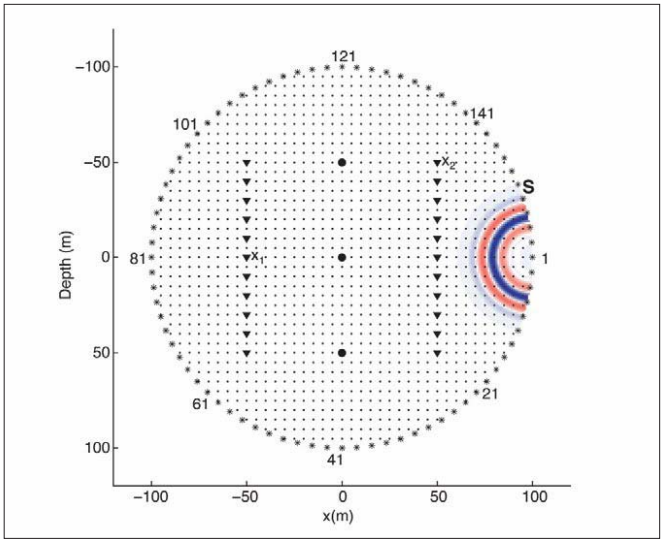

Figure 9. *Recorded impulse source in a homogeneous model. The small filled circles are point scatterers. (Figure 2, van Manen et al., "Interferometric modeling of wave propagation in inhomogeneous elastic media using time reversal and reciprocity.")*

with downward continuation, the virtual-source method (crosscorrelating traces from receiver pairs) allows for source relocation without knowledge of the complex overburden.

As demonstrated in a related article by Korneev and Bakulin (GEOPHYSICS, May-June 2006), we can think of this virtual-source method as redatuming the data to a location beneath the complex overburden by using experimentally measured information, in contrast to the traditional redatuming method that necessarily uses a coarser velocity model.

The additional resolution gained from migration of Bakulin and Calvert's virtual-source VSP data (Figure 6) reveals production-related differential compaction across the fault.

Imaging salt edge. Through VSP data, the virtual-source method is also useful for imaging a nearly vertical salt wall. Assume that we could obtain zero-offset data from a borehole in close proximity to the vertical salt face. This zero-offset data could be depth-migrated, creating an image of the salt face. As reproduced from Willis et al. (GEOPHYSICS, March-April 2006), the left-hand illustration in Figure 7 illustrates the result of this procedure applied to model data.

In contrast to the above geometry, we customarily place sources on the surface and receivers in the hole, which is the geometry of walkaway VSP. To obtain data as if the source were coincident with a downhole receiver, Willis et al. autocorrelate the VSP downhole traces for each surface source location and then sum (stack) the autocorrelations corresponding to a single subsurface receiver position but from different surface source positions. The authors use autocorrelations instead of crosscorrelations because their desired virtual-source locations are coincident with receiver locations.

This technique moves the surface source locations to the downhole virtual-source locations without knowledge of the velocity or the original source-to-receiver separation distance. The recorded first arrival at the downhole location contains the needed time-advance information. Thus, distance and velocity information are not needed.

Now for the results. Willis et al. create the central image of Figure 7 by depth-migrating the zero-offset data obtained through the autocorrelation-based virtual-source method.

Note the similarity of this image to that shown on the left.

In the July-August GEOPHYSICS supplement, Shragge et al. depth-migrate transmission data. The sources are discrete teleseismic events used to create images of the lithospheric structure. These independently distinguishable, distant-triggered events start their upward path in the lower to middle mantle. The reflections from the earth surface act as a new downward-traveling plane-wave source, which then mode-converts and reflects upward as shear waves.

Shragge et al. use the first arrival as the source in their depth migration and the later arrival as transmission/reflection events. From this, along with appropriate velocity structure, the authors image the Juan de Fuca Plate subducting underneath central Oregon (Figure 8).

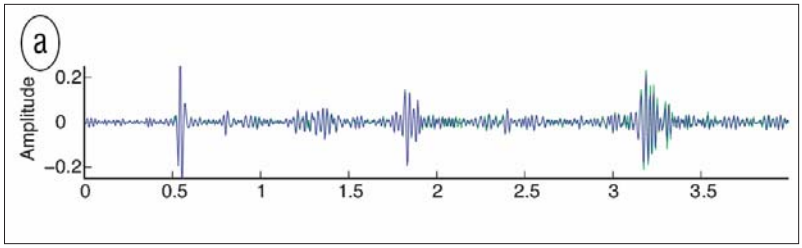

Figure 10. *Comparison of seismic traces obtained from virtual source (blue) and real source (green) at the same locations in the model. (Figure 8, van Manen et al., "Interferometric modeling of wave propagation in inhomogeneous elastic media using time reversal and reciprocity.")*

Interferometric modeling. Van Manen et al. apply interferometry to create arbitrarily sourced wavefield models. As an initial step, the authors obtain a series of model traces from receivers uniformly spaced throughout the model and a single source at the periphery of the model. Figure 9 shows an instant in a recorded wavefield in a homogeneous model that contains three point scatterers. The authors repeat this numerical experiment for each source position along the perimeter of the model. The successive source locations along the circle completely enclose the model. (Any shaped enclosure will work.)

As the second step, van Manen et al. use interferometry to create wavefields as if the source were at any location inside the circle of true sources. As is the case with the previously reported virtual-source applications, the authors generate the desired wavefields through a summation of crosscorrelations. Thus, from a series of shots around the periphery of the model, the authors construct new model traces as if there were an impulsive source at any interior location.

The collection of peripherally shot models provides a complete set of model responses and, from that, the potential to fabricate any new responses through linear superposition of those individually weighted and time-shifted models. The crosscorrelation process provides the weighting and time-shifting. The overlap of the two traces shown in Figure 10 demonstrates the success of this method in recreating a specific trace for the complex 2D elastic Pluto salt model. Because many inversion algorithms contain a modeling step, van Manen et al. suggest that their reported technique holds great promise for such inversions. TLE

—*STEPHEN J. HILL*
Colorado School of Mines, Golden, USA